

NEXT Long-Duration Test Neutralizer Performance and Erosion Characteristics

IEPC-2009-154

*Presented at the 31st International Electric Propulsion Conference,
University of Michigan • Ann Arbor, Michigan • USA
September 20 – 24, 2009*

Daniel A. Herman,^{*}
ASRC Aerospace Corporation, Cleveland, OH, 44135, United States

George C. Soulas,[†] and Michael J. Patterson[‡]
NASA Glenn Research Center, Cleveland, OH, 44135, United States

Abstract: The NASA's Evolutionary Xenon Thruster (NEXT) program is developing the next-generation ion propulsion system with significant enhancements beyond the state-of-the-art to provide future NASA science missions with enhanced capabilities at a low total development cost. A Long-Duration Test (LDT) was initiated in June 2005 to verify the NEXT propellant throughput capability to a qualification-level of 450 kg, 1.5 times the anticipated throughput requirement of 300 kg per thruster based on mission analyses. As of September 2, 2009, the thruster has accumulated 24,400 hours of operation with extensive durations at the following input powers: 6.9 kW, 4.7 kW, 1.1 kW, and 0.5 kW. The thruster has processed 434 kg of xenon, surpassing the NASA Solar Technology Application Readiness (NSTAR) program thruster propellant throughput demonstrated during the extended life testing of the Deep Space 1 flight spare ion thruster and approaching the NEXT development qualification throughput goal of 450 kg. The NEXT LDT has demonstrated a total impulse of 16.1×10^6 N·s; the highest total impulse ever demonstrated by an ion thruster. A reduction in neutralizer flow margin has been the only appreciable source of thruster performance degradation. The behavior of the neutralizer is not easily predicted due to both erosion and deposition observed in previous wear tests. Spot-to-plume mode transition flow data and in-situ erosion results for the LDT neutralizer are discussed. This loss of flow margin has been addressed through a combination of a design change in the prototype-model neutralizer to increase flow margin at low emission current and to update the NEXT throttle table to ensure adequate flow margin as a function of propellant throughput processed. The new throttle table will be used for future LDT operations. The performance of the NEXT LDT neutralizer is consistent with that observed for long-life hollow cathodes. The neutralizer life-limiting failure modes are progressing as expected and the neutralizer data indicate none of the neutralizer failures are imminent.

Nomenclature

| | |
|-------------|----------------------------------|
| <i>CCD</i> | = charge-coupled device |
| <i>DCA</i> | = discharge cathode assembly |
| <i>DCIU</i> | = digital control interface unit |
| <i>DSI</i> | = Deep Space 1 |
| <i>ELT</i> | = extended life test |

^{*} Aerospace Engineer, Propulsion and Propellants Branch, and Daniel.A.Herman@nasa.gov.

[†] Electrical Engineer, Propulsion and Propellants Branch, and George.C.Soulas@nasa.gov.

[‡] Senior Scientist, Research and Technology Directorate, and Michael.J.Patterson@nasa.gov.

| | | |
|--------------|---|---|
| <i>EM</i> | = | engineering model |
| <i>GRC</i> | = | Glenn Research Center |
| <i>IPS</i> | = | ion propulsion system |
| J_B | = | beam current, A |
| J_{NK} | = | neutralizer keeper current, A |
| m_C | = | discharge cathode flow rate, sccm |
| m_M | = | main plenum flow rate, sccm |
| m_N | = | neutralizer cathode flow rate, sccm |
| <i>LDT</i> | = | long duration test |
| <i>NCA</i> | = | neutralizer cathode assembly |
| <i>NEXT</i> | = | NASA's Evolutionary Xenon Thruster |
| <i>NSTAR</i> | = | <u>N</u> ASA <u>S</u> olar Electric Propulsion <u>T</u> echnology <u>A</u> pplication <u>R</u> eadiness |
| P_{IN} | = | thruster input power, kW |
| <i>PM</i> | = | prototype model |
| <i>PMS</i> | = | propellant management system |
| <i>PPU</i> | = | power processing unit |
| <i>QCM</i> | = | quartz-crystal microbalance |
| <i>TL</i> | = | throttle level |
| <i>TT</i> | = | throttle table |
| V_A | = | accelerator grid voltage, V |
| V_B | = | beam power supply voltage, V |
| ϕ | = | aperture or orifice diameter |

I. Introduction

THE success of the NASA Solar Electric Propulsion Technology Applications Readiness (NSTAR) ion propulsion system (IPS) on the Deep Space 1 (DS1) and Dawn missions secured the future for ion propulsion on NASA missions.¹⁻⁴ Analyses conducted at NASA identified the need for a higher-power, higher total throughput capability ion propulsion system beyond the 2.3 kW NSTAR ion thruster targeted for robotic exploration of the outer planets. The NASA's Evolutionary Xenon Thruster (NEXT) IPS, led by the NASA Glenn Research Center (GRC), is being developed to meet NASA's future mission propulsion needs for a more-advanced, higher-power IPS. NEXT performance exceeds single or multiple NSTAR thrusters over most of the thruster input power range. The wet propulsion system mass has been reduced by higher-efficiency, higher-specific impulse, and lower specific mass. With a predicted throughput capability more than double that of NSTAR, fewer NEXT thrusters are required compared to NSTAR. NEXT technology is applicable to a wide range of NASA solar system exploration missions, as well as earth-space commercial and other missions of national interest.

The NEXT system consists of a high-performance, 7 kW ion thruster; a high-efficiency, modular, 7 kW power processing unit (PPU)[§] with an efficiency and a specific power greater the NSTAR PPU; a highly-flexible, advanced xenon propellant management system (PMS)^{**} that utilizes proportional valves and thermal throttles to reduce mass and volume; a lightweight engine gimbal^{††}; and key elements of a digital control interface unit (DCIU)^{**} including software algorithms.⁵⁻¹¹ The NEXT thruster and component technologies demonstrate a significant advancement in technology beyond the state-of-the-art NSTAR thruster systems. Several key development milestones have been achieved including: environmental testing to qualification levels of engineering model hardware for the thruster and PMS; a single-string integration test of the highest fidelity (true engineering model) flight-like hardware including thruster, PMS, PPU, and DCIU simulator; a 3-string multi-thruster test on the PMS; and a 3-string multi-thruster test to characterize thruster and beam interactions.^{5,12-20} The environmental testing of the PPU is scheduled to be completed by the end of CY09. Environmental testing conditions were selected to encompass the required qualification levels for a broad range of NEXT mission applications.

Validation of the NEXT thruster service life capability is being addressed utilizing a combination of test and analyses. The NEXT thruster service life assessment was conducted at NASA GRC employing several models to evaluate all known failure modes. The assessment incorporated the results of the NEXT 2,000 h wear test (WT) conducted on a NEXT engineering model (EM) ion thruster at 6.9 kW input power.^{21,22} The assessment predicts the

[§] Power Processing Unit development led by L3 Comm ETI (Torrance, CA).

^{**} Propellant Management System and DCIU simulator development led by Aerojet (Redmond, WA).

^{††} Gimbal development led by the Jet Propulsion Laboratory and Swales Aerospace.

earliest failure occurring sometime after 750 kg of xenon throughput, well beyond the mission-derived propellant throughput requirement of 300 kg.²² To validate the NEXT thruster service life model and qualify the NEXT thruster, the NEXT Long-Duration Test (LDT) was initiated. The purposes of the NEXT LDT are to: 1) characterize thruster performance over the test duration, 2) measure the erosion rates of critical thruster components, 3) identify unknown life-limiting mechanisms, and 4) demonstrate 1.5 times the mission-derived propellant throughput requirement resulting in a qualification propellant throughput requirement of at least 450 kg. In addition to the NEXT LDT, a prototype-model thruster wear test was completed and multiple component-level lifetime tests are underway to augment the results of the LDT.²³ The NEXT thruster service life analysis is being updated based upon the LDT data and component testing findings. The thruster service life modeling is also being applied to predict thruster wear for specific trajectories from potential mission opportunities.²⁴

The results of the LDT have been discussed in numerous papers.²⁵⁻²⁷ As previously reported, the only source of appreciable degradation in the LDT thruster performance to date has been the loss of neutralizer flow margin. The spot-plume mode transition flow has been measured over the testing duration at various beam currents. Additionally, in-situ erosion characteristics of the neutralizer orifice have been obtained periodically. The neutralizer operating performance, flow margin characteristics, and erosion results will be discussed offering insight to the cause of the observed flow margin degradation. Other neutralizer life-limiting mechanisms will be evaluated based upon the LDT data obtained. Finally, the mitigation strategy to address the decreasing flow margin will be discussed.

II. Testing Hardware

A. Thruster

The NEXT LDT is being conducted with an engineering model ion thruster, designated EM3, shown in Fig. 1. The EM3 thruster has been modified to a flight-representative configuration. EM3 utilizes prototype-model (PM) ion optics manufactured by Aerojet that are flight-like and a graphite discharge cathode keeper electrode.¹⁰ The NEXT EM3 thruster, shown in Fig. 1, is nominally a 0.5 – 6.9 kW input power xenon ion thruster with dished, 2-grid ion optics. A beam extraction area 1.6 times NSTAR allows higher thruster input power while maintaining low voltages and ion current densities, thus maintaining thruster longevity. Additional description of the NEXT EM3 thruster design can be found in Refs. 26-32. Photographs of EM3 are shown in Fig. 1.

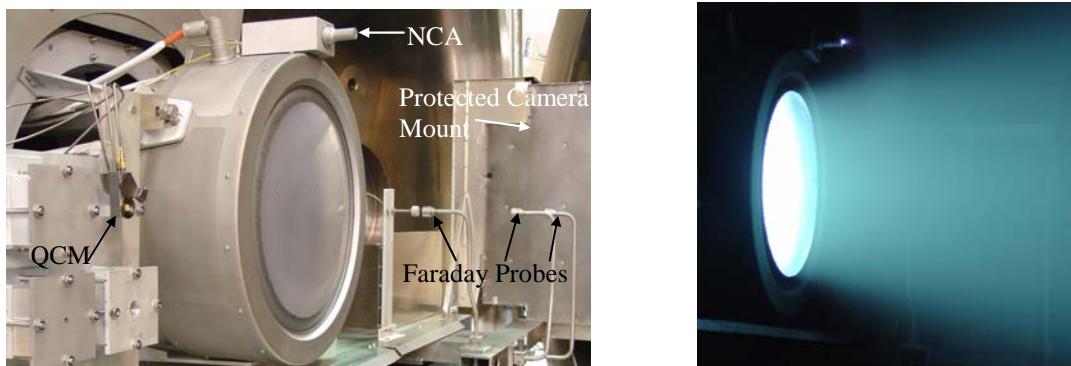


Figure 1. Photographs of the NEXT EM3 thruster: pretest photograph including diagnostic hardware (left) and photograph of operation at full-power (right).

B. NEXT Neutralizer

The neutralizer hollow cathode provides electrons to neutralize the space charge of the ion beam in order to prevent spacecraft charging. The neutralizer cathode utilizes a keeper electrode to ignite the cathode and to prevent the extinguishing of the neutralizer during thruster recycle events, i.e., when the high-voltage beam is cycled off and on. The NEXT EM3 ion thruster utilizes a neutralizer design that is mechanically similar to the Hollow Cathode Assembly of the International Space Station Plasma Contactor.³³ Because the neutralizer cathode emission current range on the NEXT ion thruster is similar to that of the Plasma Contactor Hollow Cathode Assembly, the NEXT neutralizer design can leverage the large cathode database already available with this design for risk reduction.³⁴⁻³⁷ Critical dimensions of the NEXT LDT neutralizer are identical to the prototype-model neutralizer design with the exception of a single intentional dimension change to improve flow margin at low emission current.

C. Vacuum Facility and In-situ Diagnostics

The NEXT LDT is being conducted in the 2.7 m diameter by 8.5 m long Vacuum Facility 16 (VF-16) at NASA GRC. The vacuum facility is equipped with 10 cryogenic pumps for nominal thruster operation providing a base pressure that is 3×10^{-7} Torr and a measured pumping speed, corrected for xenon, of 180 kL/s. All interior surfaces downstream of the thruster are lined with 1.2 cm thick graphite paneling to reduce the backspattered material flux to the thruster and test support hardware. The backsputter rate, nominally $3 \mu\text{m}/\text{kh}$ when the thruster is at full-power, is monitored by a quartz-crystal microbalance (QCM) positioned in the thruster exit plane at a radial position of 0.5 m from the edge of the thruster. A computerized data acquisition and control system is used to monitor and record ion engine and facility operations. Data are sampled at a frequency range of 10-20 Hz and stored every minute during normal operation. Details of the support hardware and beam diagnostics are in Refs. 21, 32, 38, and 39.

Six Sony XC-ST50 in-situ CCD cameras, shown in Fig. 2, capture the erosion patterns of critical thruster components throughout the life test. These components include the discharge cathode assembly (DCA), neutralizer cathode assembly (NCA), the downstream accelerator grid surface at three different radial locations, and the ion optics' gap between the screen and accelerator grids. The cameras are mounted to a vertical mast that is connected to a linear positioning system. Images are obtained periodically. When the cameras are not in use they are parked outside of the beam in a protective box such that there is no direct line of sight for backspattered material to deposit on the camera lenses. Each camera has a pixel cell size of $8.4 \times 9.8 \mu\text{m}$ and is fitted with an appropriate focus lens and spotlight to maximize resolution of the features of interest. Additional profile images of the neutralizer cathode assembly have been obtained by a high-resolution digital camera mounted outside the vacuum facility. These images have been obtained prior to a change in the extended operating duration throttle conditions. Additional images have been obtained while operating at low-power where the ion beam is most divergent and neutralizer keeper erosion due to the ion beam is expected to be the most severe.

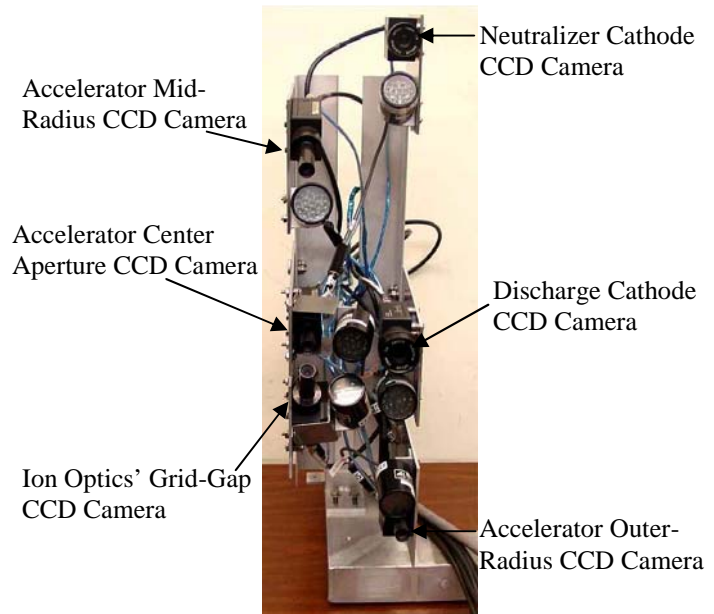


Figure 2. Erosion cameras mounted to a vertical mast.

III. Operating Conditions and Test Milestones

The NEXT IPS is designed for solar electric propulsion applications that experience variation in power available as solar flux changes at various distances from the sun throughout the mission. The IPS is designed to be throttled from 0.5 to 6.9 kW to accommodate this variation in available power. The thruster operation has been carried out in a mission-like throttling scheme with primary emphasis on wear mechanism model validation at the extremes of the NEXT throttle table. As such the thruster initially operated at full-power and has been throttled down in power, consistent with an outbound mission, with extended operations at 4 operating conditions thus far. The EM3 thruster is being operated in the NEXT LDT at discrete operating segments for extended durations to characterize erosion rates and performance as a function of time for each condition to be used in validating the thruster service life models. Long-term operating segment selections focused on operating conditions of interest with regard to wear characteristics and life-limiting phenomena. The executed/planned NEXT LDT throttling strategy is illustrated in Table 1 with completed operating segments shaded and the current operating segment in bold (1,470 hours into lowest-power segment). It is anticipated that the throttled operation will be completed by March 2010 at which point the thruster will be throttled to the operating point with the shortest lifetime, i.e., full-input power. Planned segment operating durations are subject to change if erosion or performance trends differ from projections or project/mission needs dictate. The input power indicated is a nominal operating power requirement from the NEXT throttle table at the thruster beginning-of-life and may differ slightly from thruster to thruster.²⁹ This throttling strategy demonstrates

operation over the extremes of the NEXT throttling table including: highest power (TL40), highest total accelerating voltage (TL40 and TL12), highest thermal load (TL37), condition with worst under-focusing at center-radius aperture location (TL37), condition with worst over-focusing at outer-radius locations (TL12), lowest power (TL1), lowest total accelerating voltage (TL1), lowest thermal load (TL1), most divergent beam (TL1), lowest emission currents for both hollow cathodes (TL1), and the condition with the highest ratio of discharge cathode emission to discharge cathode flow rate (TL37).

The thruster is periodically characterized over the entire throttle range covering 11 of 40 operating conditions distributed across the NEXT throttle table. Performance characterization tests are conducted to assess performance of the thruster and thruster components at multiple power levels that envelope the entire NEXT throttle table, listed in Table A1 of the Appendix. Periodic component performance assessments of the discharge chamber, ion optics, and neutralizer cathode are performed at the various thruster operating conditions.

Table 1. NEXT LDT throttling strategy. Completed segments are shaded and current segment is in bold.

| TL Level | P_{IN} , kW [†] | J_B , A | V_B , V | Duration, kh | Throughput, kg | Accumulative Throughput, kg | Total Impulse, N·s | Accumulative Total Impulse, N·s |
|----------|----------------------------|-------------|------------|--------------|----------------|-----------------------------|--------------------------------------|--------------------------------------|
| 40 | 6.86 | 3.52 | 1800 | 13.0 | 264.7 | 264.7 | 1.09×10^7 | 1.09×10^7 |
| 37 | 4.71 | 3.52 | 1180 | 6.5 | 132.6 | 397.3 | 4.45×10^6 | 1.54×10^7 |
| 5 | 1.12 | 1.20 | 679 | 3.4 | 26.7 | 424.0 | 6.30×10^5 | 1.60×10^7 |
| 1 | 0.545 | 1.00 | 275 | 3.0 | 21.2 | 445.2 | 2.75×10^5 | 1.63×10^7 |
| 12 | 2.44 | 1.20 | 1800 | 3.0 | 23.3 | 468.5 | 8.66×10^5 | 1.71×10^7 |
| Totals | | | | 28.9 | 468.5 | | 1.71×10^7 | |

[†] Nominal values

As of September 2, 2009, the NEXT EM3 thruster has accumulated 24,400 hours of operation. The NEXT thruster has processed 434 kg of xenon illustrated in Fig. 3; *surpassing the total propellant throughput processed by the DS1 flight spare in the NSTAR ELT (235 kg)*. The NEXT thruster has processed 5.9X and 1.8X the NSTAR throughput demonstrated during the DS1 mission and NSTAR ELT, respectively. Figure 3 shows the NEXT LDT propellant throughput as a function of elapsed time with reference to the NSTAR ELT and flight DS1 thruster, the thruster throughput requirements from various mission analyses conducted using the NEXT propulsion system, and the NEXT project qualification level throughput – 450 kg.⁴⁰⁻⁴² The NEXT thruster has demonstrated a total impulse of 16.1×10^6 N·s to date; *the highest total impulse ever demonstrated by an ion thruster*. The NEXT milestone is also the highest total impulse ever demonstrated by an electric propulsion device with an input power less than 10 kW.⁴³ The NEXT LDT total impulse demonstrated exceeded that of the 30,000 h NSTAR ELT in less than 1/3rd the thruster operating duration, shown in Fig. 4. Performance of the thruster has been steady with minimal degradation.

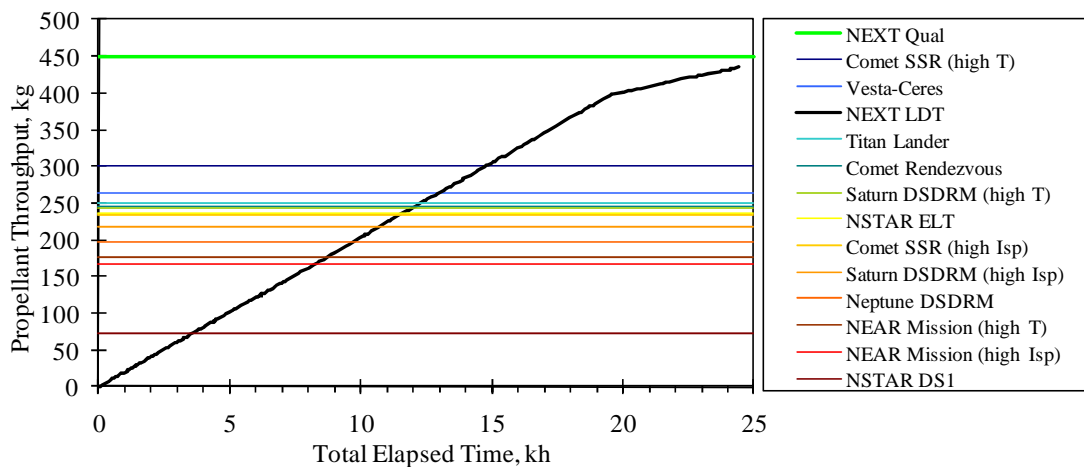


Figure 3. NEXT LDT propellant throughput data as a function of time with reference milestones.

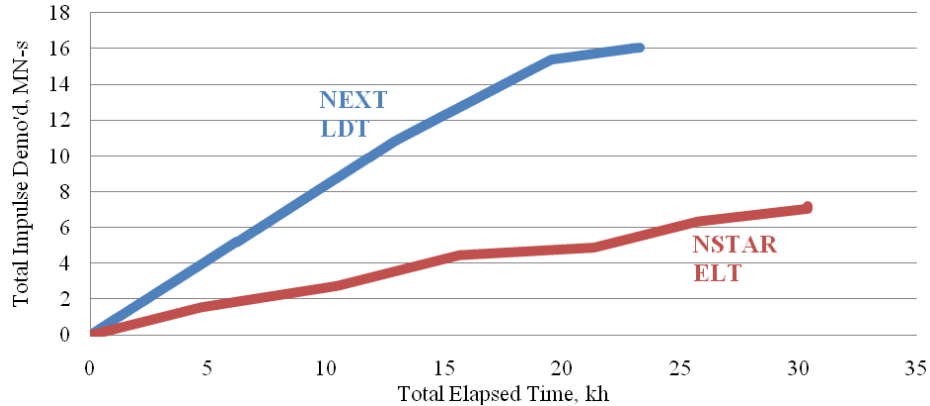


Figure 4. NEXt LDT and NSTAR ELT total impulse data as a function of time.

IV. Neutralizer Testing Results

The performance of the neutralizer cathode can be monitored via several dependent parameters that will be discussed. The neutralizer is operated with a fixed keeper current of 3 A at all operating conditions. The total neutralizer emission current is the sum of the keeper current and beam current. For a given beginning-of-life cathode geometry, the neutralizer keeper voltage is dependent upon the neutralizer mass flow rate, the beam current, the keeper current, the neutralizer internal pressure, and the geometry of the neutralizer orifice as it erodes. During the plasma contactor testing, to meet the lifetime requirements for hollow cathodes, the cathode had to be operated within controlled voltages. The operating cathode voltages, both DC and AC components, determine the emitter impacting ion energies required to self-sustain thermionic emission, but also contribute to erosion of the cathode orifice plate. The set parameters of the neutralizer are such that the emitter temperature is high enough to sustain a stable plasma, but not too high, based upon the plasma contactor development program, to reduce the cathode lifetime over the range of emission currents. Additionally, the keeper DC voltage is minimized to reduce erosion. The AC component of the keeper voltage is also important to erosion processes. The nominal operation of the neutralizer is termed spot-mode, due to the visual appearance of the plasma as a high-intensity spot residing inside the keeper orifice. Spot-mode operation is characterized by lower-voltage oscillations of the keeper voltage. Consistent with the plasma contactor and NSTAR definitions, spot-mode operation is defined as having peak-to-peak variations in keeper voltage less than 5 V. Keeper voltage oscillations greater than 5 V are defined as plume-mode operation, due to the visual appearance of the plasma as broad plume extending downstream of the keeper orifice plate. For a given emission current and orifice plate geometry, sufficient flow rate margin can preclude plume-mode operation. Over the course of the wear test, changes in neutralizer orifice geometry can affect the neutralizer internal pressure and near-field plasma, thus altering the spot-to-plume mode transition flow rate. This spot-to-plume transition flow has been measured throughout the course of the NEXt LDT.

Several life-limiting modes exist for the neutralizer including: cathode orifice erosion, cathode orifice clogging, keeper tube erosion due to high-energy ion impingement, barium depletion of the emitter, failure to ignite, heater failure, and loss of impedance between the keeper and cathode common. Energetic ion production due to plume-mode operation can accelerate the progression of several of these failure modes.

A. Neutralizer Ignitions and Heater Performance

The swaged heater cyclic lifetime was established during the ISS plasma contactor development.⁴⁴ The cyclic heater testing of three plasma contactor heaters to failure established an estimated B_{10} lifetime (number of cycles in which 10% of all heaters would have failed) of 6,679 cycles via a Weibull analysis. The heater cycle profile was 6 minutes powered at 8.50 A (in power-limited mode) then 4 minutes unpowered. If the NEXt LDT neutralizer ignition durations are less than 6 minutes, the ISS plasma contactor heater cyclic lifetime is portable to the NEXt neutralizer. The LDT neutralizer ignition durations are plotted as a function of time in Fig. 5 with all ignition durations less than 6 minutes. The largest ignition duration followed a 6 month test downtime to decontaminate the facility cryo-pumps of oil. Hard vacuum was maintained throughout via 2 operating cryo-pumps. Typical ignition durations are less than 4 minutes with most occurring immediately after the neutralizer keeper power supply and igniter circuit are powered, i.e., at 3.5 minutes.

Heater operational performance is determined by monitoring the heater voltage after 3.50 minutes of 8.50 A heater current (in fixed current mode). Heater voltage during the ISS plasma contactor cyclic testing indicated an increasing heater voltage due to extended time at high temperature that changes the material properties of the heating element wire. Prior to heater failure, a change in slope of the heater voltage at the end of cycle (voltage runoff) was observed.⁴⁴ The NEXT LDT neutralizer heater voltage after 3.50 minutes of heater current is shown as a function of neutralizer ignition in Fig. 6. A gradual increase in the heater voltage of 2% is observed after 207 neutralizer ignitions. This modest increase in heater voltage is consistent with the trends for long-life heater operation and does not indicate voltage runoff. Additionally, heater failure is unlikely given the modest cyclic requirements for life testing (3% of heater cyclic B₁₀ life consumed to date) and typical NEXT IPS applications.

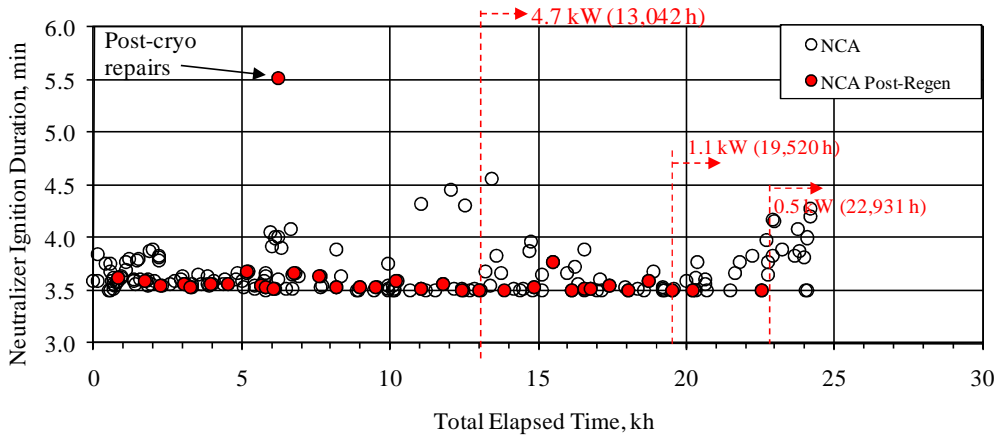


Figure 5. Neutralizer ignition durations: 8.50 A heater current applied.

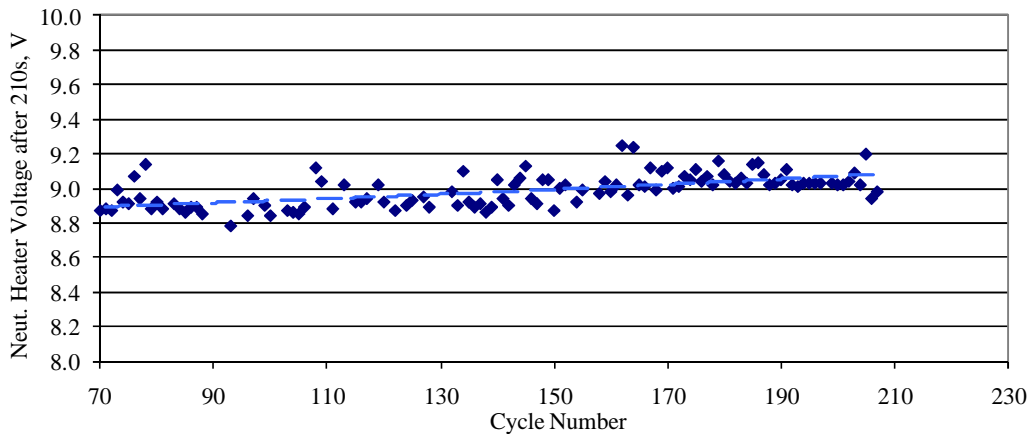


Figure 6. LDT neutralizer heater voltage after 3.50 minutes of heater current.

B. Neutralizer Performance

Neutralizer keeper voltage, relative to neutralizer cathode common, and the coupling voltage between neutralizer cathode common and the vacuum facility ground are shown in Fig. 7. The keeper voltage has demonstrated a slight decrease over 19.5 kh during which it was operated at fixed emission current and flow rate.²⁷ The neutralizer keeper voltage decreased from 11.2 to 10.7 volts during the first 10 kh at full-power. This minor decrease is likely due to erosion of the neutralizer cathode orifice plate. A decreasing nominal keeper voltage of similar magnitude was observed at full-power during the NSTAR ELT as well.^{42,45} The coupling voltage was steady at $-10.2 \text{ V} \pm 0.2 \text{ V}$ during the first 19.5 kh. Spikes in the keeper and coupling voltages are due to thruster shutdown and restart events where steady-state conditions do not exist for the neutralizer. Upon transitioning to different throttling conditions, the keeper and coupling voltages quickly settle in on fixed values, though higher variability in both parameters is observed. This variability of $\pm 0.25 \text{ V}$ for fixed operating conditions is considerably less than those observed in

NSTAR ELT neutralizer cathode where the variations on the order of a volt are evident in the keeper voltage.^{42,45} The application of a two-dimensional axisymmetric model of the plasma and neutral gas in electric propulsion hollow cathodes for the NEXT LDT neutralizer reveals that the erosion of the cathode orifice is sufficient to cause the observed keeper voltage drop with time.⁴⁶ While in-situ cameras image the neutralizer orifice, the measurement indicates the minimum orifice channel diameter. Detailed erosion orifice geometry as a function of axial distance cannot be determined using the NEXT LDT cameras. Post-test measurements will be made.

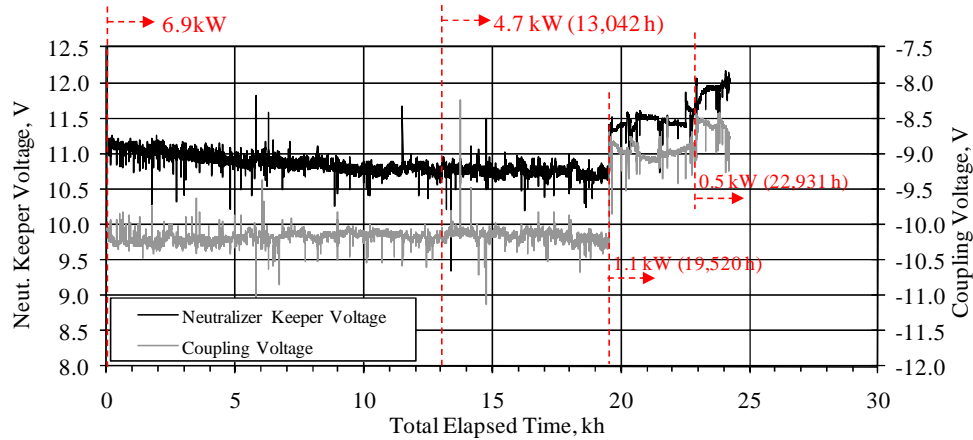


Figure 7. Neutralizer keeper voltage and coupling voltage as a function of LDT test duration with transitions of runtime operating conditions indicated.

A NEXT technology development throttle table was established and iterated as the program progressed. At the initiation of the NEXT LDT, a throttle table had been used as the baseline for thruster control parameters. The throttle table, TT9, was based upon performance testing of engineering model thrusters. The set parameters for accelerator grid voltage and neutralizer flow rate were intended to give sufficient margin to prevent electron backstreaming and spot-to-plume mode transition, respectively, as the thruster wears. These margins were based upon the NEXT EM 2 kh wear test and NSTAR wear tests. Throttle table 9, Table A1, was also used as the basis for the NEXT thruster service life assessment. Relative to the NEXT technology development throttle table at the inception of the NEXT LDT (TT9), a loss in neutralizer flow margin has been observed, as shown in Figure 8. Loss of neutralizer flow margin at low emission currents was also observed during the NSTAR ELT, though this occurred during a time when deposits were forming and clogging the neutralizer orifice.^{42,45} From the NSTAR ELT at full-power, where plume-mode was reached during characterizations throughout the test, the full-power flow margin decreased by 0.5 sccm over 29 kh.^{42,45} Over the same amount of propellant throughput, the NEXT LDT full-power flow margin has decreased by 0.7 sccm.

As Fig. 8 illustrates, there is considerable flow margin at the high beam (i.e., high neutralizer emission current) current operating conditions. Transition flow margin has decreased, based on beginning-of-life neutralizer flow rates, for all beam current conditions over the test duration. Motivated by the EM neutralizer low flow margin at beginning-of-life, design modifications have been incorporated into the PM neutralizer design yielding higher flow margin at low-power with the modest expense of $\sim 1V$ increase in the magnitude of the coupling voltage.⁵ The beginning-of-life flow margins for the first NEXT PM thruster are shown in Fig. 9. The effect of the neutralizer design change is improved flow margin for beam currents less than 2.70 A, slightly decrease flow margins for beam currents above 2.70 A, and no change in flow margin for 2.70 A beam current.

The NEXT throttle table was updated based on the changes in LDT neutralizer flow margin as a function of propellant throughput processed and the changes in neutralizer flow margin for the prototype-model neutralizer. The new throttle table (TT10), shown in Table A2 and Table A3, contain the NEXT beginning-of-life operating parameters and neutralizer flow rates as a function of processed propellant throughput, respectively. The neutralizer flow rate increases account for the observed degradation experienced during the LDT. Minor changes to accelerator grid voltages are also included to take advantage of the improved perveance of the prototype-model ion optics. Throttle table 10 is now the baseline throttle table for the technology program and for mission analyses. The impact of the neutralizer flow increases on IPS performance is mission specific depending upon the throttling profile dictated by the mission trajectory. For the LDT throttling profile, given in Table 1, the new neutralizer flows will result in a negligible increase of 3.5 kg of xenon processed, which is 0.75% of the total throughput processed.

Figure 10 illustrates the adjusted NEXT LDT flow margin assuming throttle table 10 neutralizer flow rates and the beginning-of-life change in flow margin for prototype-model neutralizer design. As illustrated in Fig. 10, NEXT TT10 ensures adequate neutralizer flow margin for the prototype-model neutralizer design as the neutralizer orifice erodes. Additional resources are being applied to predict the spot-to-plume mode transition flow using the Orificed Cathode two-dimensional (OrCa2D) computer code.^{47,48} The goal of this modeling would be to predict the change in flow margin as a function of operating condition based upon an input neutralizer eroded orifice geometry.⁴⁶

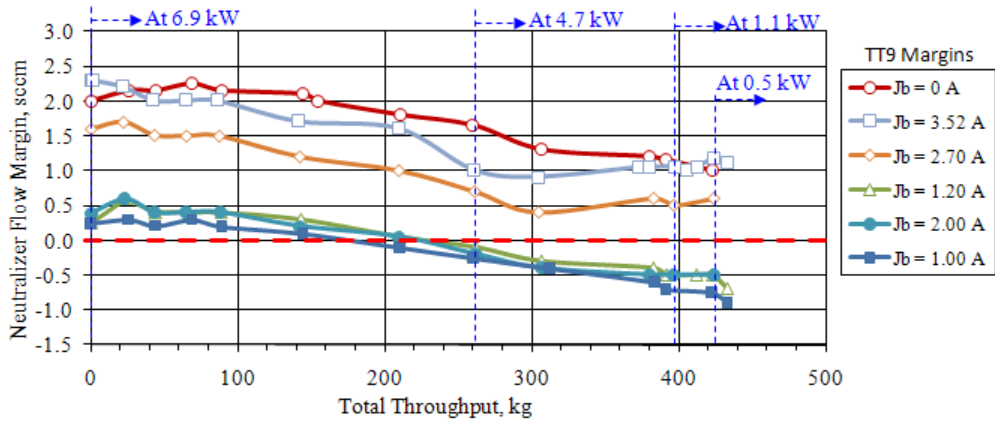


Figure 8. Neutralizer flow margins based on NEXT throttle table 9 (TT9).

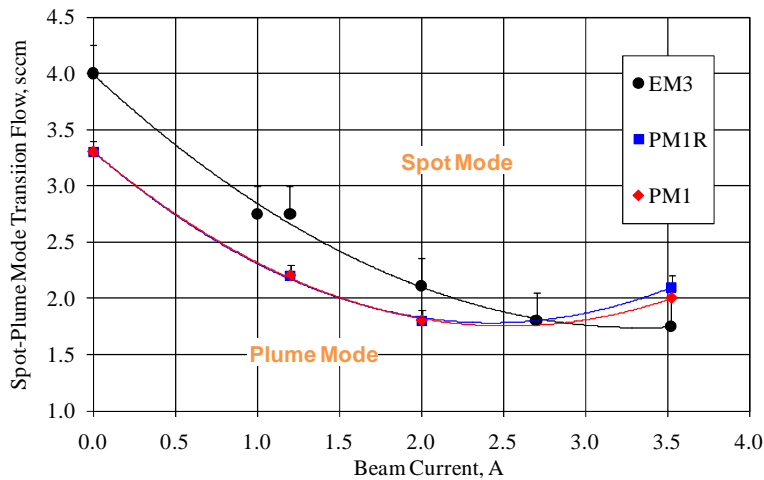


Figure 9. Neutralizer spot-to-plume transition flow for the LDT (EM3) and PM neutralizer cathodes.

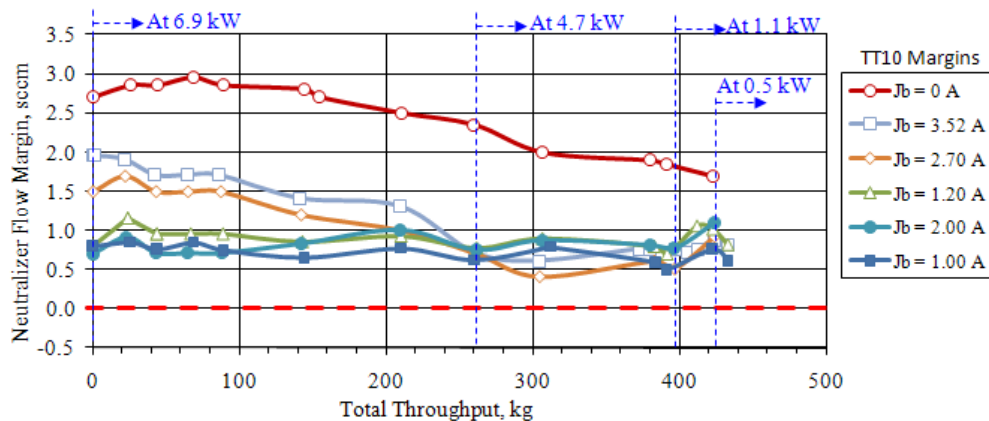


Figure 10. Anticipated neutralizer flow margin based on NEXT throttle table 10 (TT10) inputs and PM neutralizer design improvements as a function of propellant throughput for various beam currents.

The physics that drive a cathode into plume mode are not well understood, but the erosion of the cathode orifice is assumed to contribute to the loss of the neutralizer flow margin. If erosion of the neutralizer orifice leads to loss of flow margin it is expected that the neutralizer internal pressure would also change due to the erosion. A 100 Torr capacitance manometer mounted downstream of the neutralizer mass flow controller is used to monitor the neutralizer internal pressure. There is an estimated 15' of propellant line length from the capacitance manometer to the neutralizer, thus the data presented is corrected for the pressure drop due to viscosity effects using the Darcy-Weisbach equation for compressible flows. Figure 11 details the corrected neutralizer pressure since 16 kh, i.e., during the 4.7 kW run segment. At 4.7 kW, a 4% decrease in neutralizer pressure is observed over approximately 3,300 hours of operation at 6.52 A neutralizer emission current. This decreasing neutralizer pressure is likely a result of the neutralizer orifice erosion and the main contributor to the loss of flow margin. However, measurement of the neutralizer cold flow over the same duration indicates no change in cold-flow neutralizer pressure within the measurement accuracy. Though the 100 Torr capacitance manometer is not ideal to measure cold flow pressure variations whose nominal value is on the order of 10 Torr. The magnitude of the neutralizer pressure at 16 kh, indicates that considerable degradation in pressure had already occurred, consistent with the loss of flow margin. After throttling to lower-power and lower neutralizer emission currents, there has been no observed change in the operating neutralizer pressure for these operating conditions. Note that the sporadically high data points observed in Fig. 11 are during thruster restarts where the neutralizer flow without beam extraction is set to 6.00 sccm thus building up the neutralizer internal pressure. When the high-voltage is applied, the neutralizer flow is decreased to the set value, yet the internal pressure takes time to bleed down to its nominal value.

Data obtained on the PM1R thruster during acceptance testing indicate a full-power beginning-of-life neutralizer pressure of 68 Torr (data obtained with a pressure tap just upstream of the neutralizer cathode). The PM1R thruster wear test recorded an approximately 25% decrease in the neutralizer inlet pressure over 1350 hours of operation.⁴⁹ A leak was found post-test in the propellant tubing leading to the neutralizer that could have contributed to the pressure decrease, shown in Fig. 12. Pre-wear test pressure data obtained on PM1R indicated an internal pressure that was ~10 Torr higher than the beginning of the PM1R wear test. The tubing leak likely contributed to this ~10 Torr shift from acceptance testing to the beginning of the wear test. Though a leak was found post-test for the PM1R wear test, the beginning of life neutralizer pressures measured from multiple NEXT tests indicate that a significant pressure drop in the LDT neutralizer has occurred prior to recording of the neutralizer pressure data. Neutralizer pressure behavior similar to that observed during the PM1R wear test is expected even though the magnitude of the leak and its impact on the pressure data could not be quantified.

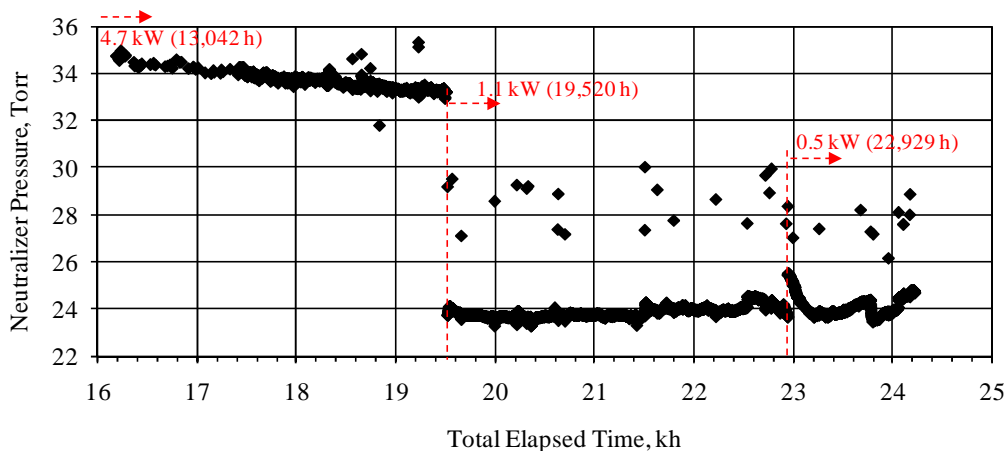


Figure 11. Neutralizer pressure (corrected for pressure drop) during NEXT LDT as a function of time.

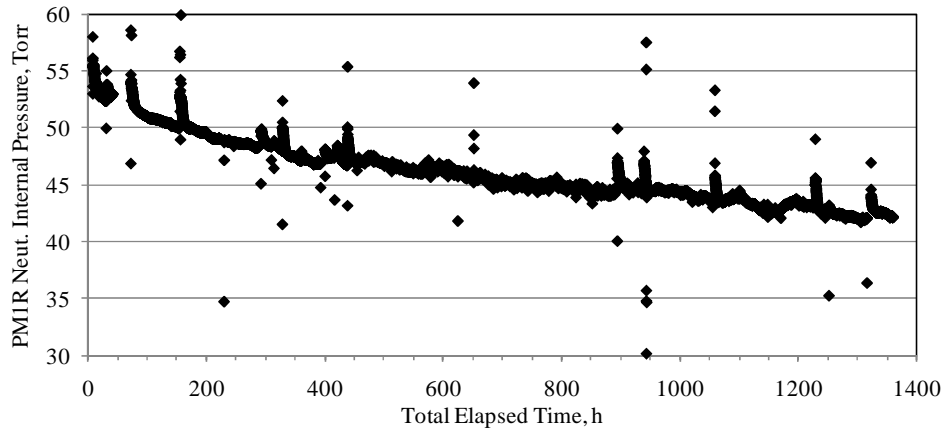


Figure 12. Neutralizer inlet pressure as a function of time during the PMIR wear test.

D. Neutralizer Cathode Assembly (NCA) Erosion

Prior to the start of the NEXT LDT, detailed geometric measurements were made of the neutralizer cathode assembly. These measurements included laser profilometer measurements of the keeper orifice plates and pin gauges of the hollow cathode orifice diameters. Pretest photographs documenting the condition of the neutralizer assembly are shown in Fig. 13. In-situ images of the neutralizer face plates and keeper tube have been obtained periodically throughout the test for comparison to the pretest conditions.

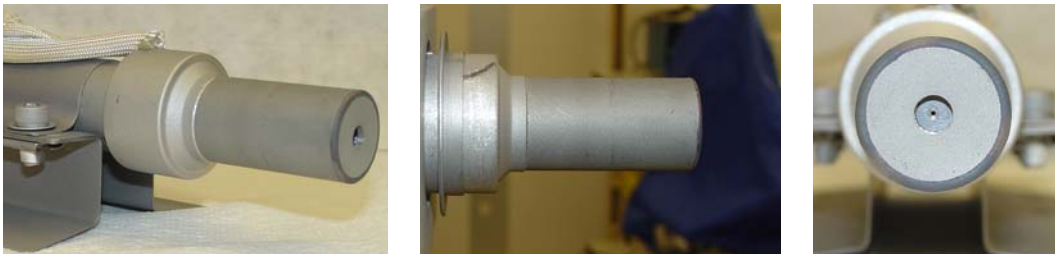


Figure 13. Neutralizer cathode pretest photographs during thruster assembly.

Figure 14 shows the neutralizer cathode assembly pretest and image taken after 24,400 h of thruster operation. Texturing of the neutralizer cathode faceplate is observed and a darkening of the keeper is seen due to backspattered carbon deposition from the facility. The NCA is located in the 12 o'clock position of the thruster so any erosion due to placement of the NCA in the high-energy beam would be seen in the bottom of the images taken, which appears pristine. Normalized measurements from the erosion images, shown in Fig. 15, confirm no observed erosion of the NCA keeper orifice diameter or cathode orifice minimum diameter, while the cathode orifice chamfer diameter, i.e., the maximum diameter of the conical section of the orifice, has increased by ~20% over the test duration. No clogging of the neutralizer orifice has been observed even at the lowest neutralizer emission currents.

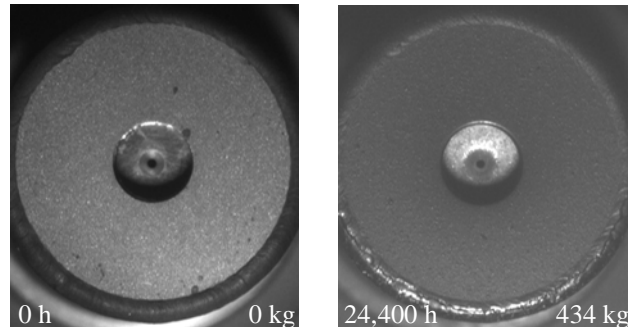


Figure 14. Neutralizer assembly erosion images.

Though the neutralizer minimum orifice diameter does not show any erosion when imaging on centerline, it is likely that the EM3 neutralizer orifice channel has eroded. Post-test neutralizer orifice channel erosion profiles were measured after the NSTAR 8,200 h wear test and NSTAR ELT indicating a bell-shaped erosion pattern with minimal erosion of the upstream diameter, but the channel width increases towards the keeper.^{42,47,50} The observed reduction in neutralizer flow margin and neutralizer internal pressure with the NEXT LDT test duration suggests erosion of the orifice channel is occurring.²⁷

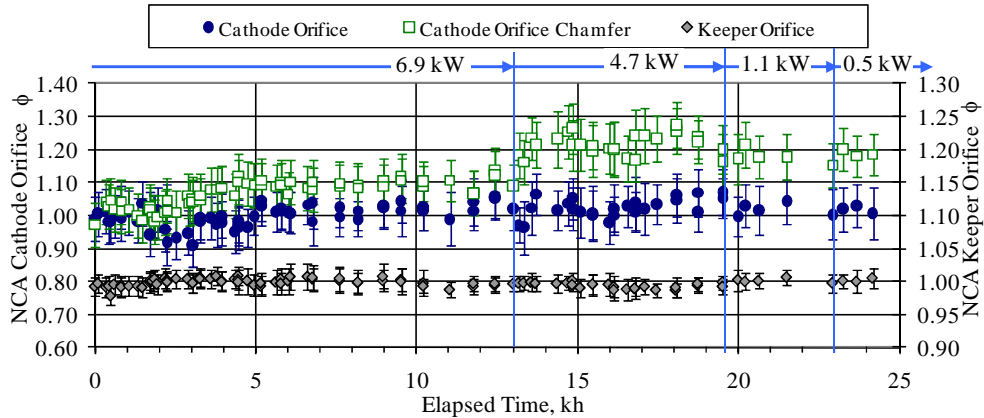


Figure 15. Neutralizer cathode minimum orifice diameter, orifice chamfer diameter, and keeper orifice diameter normalized to pretest values as a function of time.

The erosion of the keeper tube of the neutralizer due to direct ion impingement is also of concern for extended ion thruster operations. This is of particular interest for low-power operating conditions in which the ion beam is the most divergent. Profile images of the keeper tube obtained during the LDT are consistent with images of the front face of the neutralizer indicating the lack of any appreciable erosion of the keeper faceplate, i.e., the faceplate weld appears pristine. Figure 16 documents the lack of appreciable erosion on the neutralizer keeper tube over the test duration. The bottom of the keeper tube does have some slight discoloration due to ion impingement, but the keeper tube does not show increased or concerning erosion at the lowest-power, most divergent operating point.

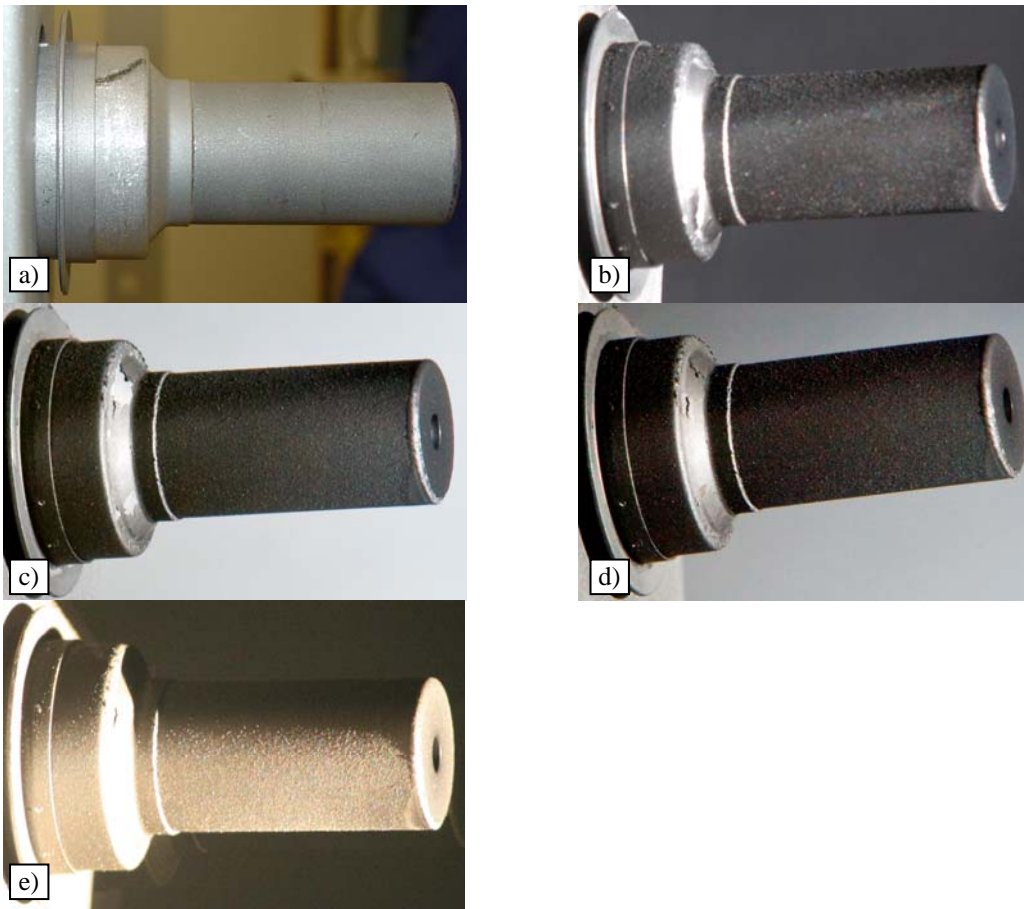


Figure 16. Neutralizer keeper photographs: a) pretest, b) after 6.9 kW run segment, c) after 4.7 kW run segment, d) after 1.1 kW run segment, and e) 1,245 hours into 0.5 kW run segment.

V. Conclusion

The status of the NEXT Long-Duration Test (LDT) as of September 2, 2009 was presented. The NEXT EM3 thruster has accumulated 24,400 h of operation, processed 434 kg of xenon, and demonstrated a total impulse of 16.1×10^6 N·s. *The NEXT thruster has surpassed the total throughput (1.8X) demonstrated by any ion thruster including the NSTAR flight spare thruster. The NEXT LDT total impulse is the highest ever demonstrated by an ion thruster.*

Neutralizer ignition durations are typically within 4 minutes and all are within the 6 minute qualification testing duration. Neutralizer heater voltages at temperature have risen slightly as expected, but give no indication of voltage runoff. This is expected since the number of heater cycles thus far is only 3% of the established, flight qualified B₁₀ life for the neutralizer heater. A decrease in the neutralizer spot-to-plume mode transition flow margin has been the only appreciable source of thruster performance degradation during the NEXT LDT. Though minimal erosion of the neutralizer cathode orifice plate or keeper tube has been detected, the loss of flow margin and measured decrease in neutralizer internal pressure indicate the neutralizer orifice channel is likely eroding. Recent, physics-based numerical simulations also support this conclusion. Neutralizer orifice channel erosion was expected based upon previous ion thruster wear tests. The modest decrease in keeper voltage with operating duration at full-power is consistent with the NSTAR ELT trends. Two-dimensional axisymmetric modeling of the plasma and neutral gas in the neutralizer supports the observation that the trend can be attributed to orifice channel erosion.

The loss of flow margin has been addressed by prototype-model neutralizer design modifications and updating the NEXT throttle table (TT10) with higher neutralizer flows as a function of propellant throughput processed. These changes are predicted to ensure a minimum neutralizer flow margin of 0.4 sccm for all operating conditions as the thruster wears. The impact of the increase in neutralizer flow as a function of propellant throughput processed is mission specific, requiring detailed knowledge of individual thruster throttling profiles. Based upon the LDT throttling profile outlined, the increased neutralizer flows will result in a negligible propellant penalty of 3.5 kg of xenon out of the anticipated 468.5 kg processed (0.75% of the total propellant throughput).

The NEXT LDT is gradually progressing towards, and soon will demonstrate, the project qualification throughput of 450 kg propellant throughput. The prototype-model neutralizer dimension change and new TT10 neutralizer flows ensure adequate neutralizer flow margin to maintain spot-mode operation as the orifice channel erodes throughout the thruster's lifetime. Throttle table 10 will be the source of thruster control parameters for the remainder of the NEXT LDT and technology development program.

Appendix

Table A1. NEXT throttle table 9 (TT9) with LDT performance operating conditions subset shaded. Full-power wear test condition in bold. Input powers are beginning-of-life values.

| TL Level | P_{IN} , kW [†] | J_B , A | V_B , V | V_A , V | m_M , sccm | m_C , sccm | m_N , sccm | J_{NK} , A |
|-----------|----------------------------|-------------|-------------|-------------|--------------|--------------|--------------|--------------|
| 40 | 6.83 | 3.52 | 1800 | -210 | 49.6 | 4.87 | 4.01 | 3.00 |
| 39 | 6.03 | 3.52 | 1570 | -210 | 49.6 | 4.87 | 4.01 | 3.00 |
| 38 | 5.43 | 3.52 | 1400 | -210 | 49.6 | 4.87 | 4.01 | 3.00 |
| 37 | 4.68 | 3.52 | 1180 | -200 | 49.6 | 4.87 | 4.01 | 3.00 |
| 36 | 6.03 | 3.10 | 1800 | -210 | 43.5 | 4.54 | 4.01 | 3.00 |
| 35 | 5.32 | 3.10 | 1570 | -210 | 43.5 | 4.54 | 4.01 | 3.00 |
| 34 | 4.80 | 3.10 | 1400 | -210 | 43.5 | 4.54 | 4.01 | 3.00 |
| 33 | 4.14 | 3.10 | 1180 | -200 | 43.5 | 4.54 | 4.01 | 3.00 |
| 32 | 5.27 | 2.70 | 1800 | -210 | 37.6 | 4.26 | 3.50 | 3.00 |
| 31 | 4.65 | 2.70 | 1570 | -210 | 37.6 | 4.26 | 3.50 | 3.00 |
| 30 | 4.19 | 2.70 | 1400 | -210 | 37.6 | 4.26 | 3.50 | 3.00 |
| 29 | 3.61 | 2.70 | 1180 | -200 | 37.6 | 4.26 | 3.50 | 3.00 |
| 28 | 3.20 | 2.70 | 1020 | -175 | 37.6 | 4.26 | 3.50 | 3.00 |
| 27 | 4.60 | 2.35 | 1800 | -210 | 32.4 | 4.05 | 3.50 | 3.00 |
| 26 | 4.06 | 2.35 | 1570 | -210 | 32.4 | 4.05 | 3.50 | 3.00 |
| 25 | 3.66 | 2.35 | 1400 | -210 | 32.4 | 4.05 | 3.50 | 3.00 |
| 24 | 3.16 | 2.35 | 1180 | -200 | 32.4 | 4.05 | 3.50 | 3.00 |
| 23 | 2.80 | 2.35 | 1020 | -175 | 32.4 | 4.05 | 3.50 | 3.00 |
| 22 | 4.00 | 2.00 | 1800 | -210 | 25.8 | 3.87 | 2.50 | 3.00 |
| 21 | 3.54 | 2.00 | 1570 | -210 | 25.8 | 3.87 | 2.50 | 3.00 |
| 20 | 3.20 | 2.00 | 1400 | -210 | 25.8 | 3.87 | 2.50 | 3.00 |
| 19 | 2.77 | 2.00 | 1180 | -200 | 25.8 | 3.87 | 2.50 | 3.00 |
| 18 | 2.46 | 2.00 | 1020 | -175 | 25.8 | 3.87 | 2.50 | 3.00 |
| 17 | 3.24 | 1.60 | 1800 | -210 | 20.0 | 3.70 | 2.75 | 3.00 |
| 16 | 2.87 | 1.60 | 1570 | -210 | 20.0 | 3.70 | 2.75 | 3.00 |
| 15 | 2.60 | 1.60 | 1400 | -210 | 20.0 | 3.70 | 2.75 | 3.00 |
| 14 | 2.26 | 1.60 | 1180 | -200 | 20.0 | 3.70 | 2.75 | 3.00 |
| 13 | 2.01 | 1.60 | 1020 | -175 | 20.0 | 3.70 | 2.75 | 3.00 |
| 12 | 2.43 | 1.20 | 1800 | -210 | 14.2 | 3.57 | 3.00 | 3.00 |
| 11 | 2.15 | 1.20 | 1570 | -210 | 14.2 | 3.57 | 3.00 | 3.00 |
| 10 | 1.95 | 1.20 | 1400 | -210 | 14.2 | 3.57 | 3.00 | 3.00 |
| 9 | 1.70 | 1.20 | 1180 | -200 | 14.2 | 3.57 | 3.00 | 3.00 |
| 8 | 1.51 | 1.20 | 1020 | -175 | 14.2 | 3.57 | 3.00 | 3.00 |
| 7 | 1.41 | 1.20 | 936 | -150 | 14.2 | 3.57 | 3.00 | 3.00 |
| 6 | 1.31 | 1.20 | 850 | -125 | 14.2 | 3.57 | 3.00 | 3.00 |
| 5 | 1.11 | 1.20 | 679 | -115 | 14.2 | 3.57 | 3.00 | 3.00 |
| 4 | 1.08 | 1.20 | 650 | -144 | 14.2 | 3.57 | 3.00 | 3.00 |
| 3 | 0.777 | 1.20 | 400 | -394 | 14.2 | 3.57 | 3.00 | 3.00 |
| 2 | 0.656 | 1.20 | 300 | -525 | 14.2 | 3.57 | 3.00 | 3.00 |
| 1 | 0.529 | 1.00 | 275 | -500 | 12.3 | 3.52 | 3.00 | 3.00 |

[†] Nominal values at beginning of life

Table A2. NEXT beginning-of-life throttle table (TT10) with LDT performance operating conditions subset shaded. Full-power wear test condition in bold.

| TL Level | P_{IN} , kW [†] | J_B , A | V_B , V | V_A , V | m_M , sccm | m_C , sccm | m_N , sccm | J_{NK} , A |
|-----------|----------------------------|-------------|-------------|-------------|--------------|--------------|--------------|--------------|
| 40 | 6.86 | 3.52 | 1800 | -210 | 49.6 | 4.87 | 4.01 | 3.00 |
| 39 | 6.05 | 3.52 | 1570 | -210 | 49.6 | 4.87 | 4.01 | 3.00 |
| 38 | 5.46 | 3.52 | 1400 | -210 | 49.6 | 4.87 | 4.01 | 3.00 |
| 37 | 4.71 | 3.52 | 1180 | -200 | 49.6 | 4.87 | 4.01 | 3.00 |
| 36 | 6.06 | 3.10 | 1800 | -210 | 43.5 | 4.54 | 4.01 | 3.00 |
| 35 | 5.35 | 3.10 | 1570 | -210 | 43.5 | 4.54 | 4.01 | 3.00 |
| 34 | 4.82 | 3.10 | 1400 | -210 | 43.5 | 4.54 | 4.01 | 3.00 |
| 33 | 4.14 | 3.10 | 1180 | -200 | 43.5 | 4.54 | 4.01 | 3.00 |
| 32 | 5.29 | 2.70 | 1800 | -210 | 37.6 | 4.26 | 3.50 | 3.00 |
| 31 | 4.67 | 2.70 | 1570 | -210 | 37.6 | 4.26 | 3.50 | 3.00 |
| 30 | 4.22 | 2.70 | 1400 | -210 | 37.6 | 4.26 | 3.50 | 3.00 |
| 29 | 3.64 | 2.70 | 1180 | -200 | 37.6 | 4.26 | 3.50 | 3.00 |
| 28 | 3.22 | 2.70 | 1020 | -175 | 37.6 | 4.26 | 3.50 | 3.00 |
| 27 | 4.62 | 2.35 | 1800 | -210 | 32.4 | 4.05 | 3.50 | 3.00 |
| 26 | 4.08 | 2.35 | 1570 | -210 | 32.4 | 4.05 | 3.50 | 3.00 |
| 25 | 3.68 | 2.35 | 1400 | -210 | 32.4 | 4.05 | 3.50 | 3.00 |
| 24 | 3.18 | 2.35 | 1180 | -200 | 32.4 | 4.05 | 3.50 | 3.00 |
| 23 | 2.82 | 2.35 | 1020 | -175 | 32.4 | 4.05 | 3.50 | 3.00 |
| 22 | 4.01 | 2.00 | 1800 | -210 | 25.8 | 3.87 | 2.50 | 3.00 |
| 21 | 3.54 | 2.00 | 1570 | -210 | 25.8 | 3.87 | 2.50 | 3.00 |
| 20 | 3.21 | 2.00 | 1400 | -210 | 25.8 | 3.87 | 2.50 | 3.00 |
| 19 | 2.78 | 2.00 | 1180 | -200 | 25.8 | 3.87 | 2.50 | 3.00 |
| 18 | 2.47 | 2.00 | 1020 | -175 | 25.8 | 3.87 | 2.50 | 3.00 |
| 17 | 3.25 | 1.60 | 1800 | -210 | 20.0 | 3.70 | 2.75 | 3.00 |
| 16 | 2.88 | 1.60 | 1570 | -210 | 20.0 | 3.70 | 2.75 | 3.00 |
| 15 | 2.61 | 1.60 | 1400 | -210 | 20.0 | 3.70 | 2.75 | 3.00 |
| 14 | 2.27 | 1.60 | 1180 | -200 | 20.0 | 3.70 | 2.75 | 3.00 |
| 13 | 2.02 | 1.60 | 1020 | -175 | 20.0 | 3.70 | 2.75 | 3.00 |
| 12 | 2.44 | 1.20 | 1800 | -210 | 14.2 | 3.57 | 3.00 | 3.00 |
| 11 | 2.16 | 1.20 | 1570 | -210 | 14.2 | 3.57 | 3.00 | 3.00 |
| 10 | 1.96 | 1.20 | 1400 | -210 | 14.2 | 3.57 | 3.00 | 3.00 |
| 9 | 1.70 | 1.20 | 1180 | -200 | 14.2 | 3.57 | 3.00 | 3.00 |
| 8 | 1.52 | 1.20 | 1020 | -175 | 14.2 | 3.57 | 3.00 | 3.00 |
| 7 | 1.42 | 1.20 | 936 | -150 | 14.2 | 3.57 | 3.00 | 3.00 |
| 6 | 1.32 | 1.20 | 850 | -125 | 14.2 | 3.57 | 3.00 | 3.00 |
| 5 | 1.12 | 1.20 | 679 | -115 | 14.2 | 3.57 | 3.00 | 3.00 |
| 4 | 1.09 | 1.20 | 650 | -144 | 14.2 | 3.57 | 3.00 | 3.00 |
| 3 | 0.789 | 1.20 | 400 | -310 | 14.2 | 3.57 | 3.00 | 3.00 |
| 2 | 0.669 | 1.20 | 300 | -410 | 14.2 | 3.57 | 3.00 | 3.00 |
| 1 | 0.545 | 1.00 | 275 | -350 | 12.3 | 3.52 | 3.00 | 3.00 |

[†] Nominal values at beginning of life

Table A3. NEXT throttle table (TT10) neutralizer flow rate set point as a function of propellant throughput for fixed neutralizer keeper current of 3.00 A. NEXT LDT performance operating conditions subset shaded. Full-power wear test condition in bold. After each throughput milestone is surpassed, the new flow rate becomes the set point.

| TL Level | P _{IN} , kW [†] | J _B , A | Neutralizer flow rate (m _N), sccm | | | | | |
|-----------|-----------------------------------|--------------------|---|-------------|-------------|-------------|-------------|-------------|
| | | | 0 kg | 100 kg | 200 kg | 300 kg | 400 kg | 450 kg |
| 40 | 6.86 | 3.52 | 4.01 | 4.01 | 4.01 | 4.01 | 4.01 | 4.33 |
| 39 | 6.05 | 3.52 | 4.01 | 4.01 | 4.01 | 4.01 | 4.01 | 4.33 |
| 38 | 5.46 | 3.52 | 4.01 | 4.01 | 4.01 | 4.01 | 4.01 | 4.33 |
| 37 | 4.71 | 3.52 | 4.01 | 4.01 | 4.01 | 4.01 | 4.01 | 4.33 |
| 36 | 6.06 | 3.10 | 4.01 | 4.01 | 4.01 | 4.01 | 4.01 | 4.33 |
| 35 | 5.35 | 3.10 | 4.01 | 4.01 | 4.01 | 4.01 | 4.01 | 4.33 |
| 34 | 4.82 | 3.10 | 4.01 | 4.01 | 4.01 | 4.01 | 4.01 | 4.33 |
| 33 | 4.14 | 3.10 | 4.01 | 4.01 | 4.01 | 4.01 | 4.01 | 4.33 |
| 32 | 5.29 | 2.70 | 3.50 | 3.50 | 3.50 | 3.50 | 3.82 | 4.14 |
| 31 | 4.67 | 2.70 | 3.50 | 3.50 | 3.50 | 3.50 | 3.82 | 4.14 |
| 30 | 4.22 | 2.70 | 3.50 | 3.50 | 3.50 | 3.50 | 3.82 | 4.14 |
| 29 | 3.64 | 2.70 | 3.50 | 3.50 | 3.50 | 3.50 | 3.82 | 4.14 |
| 28 | 3.22 | 2.70 | 3.50 | 3.50 | 3.50 | 3.50 | 3.82 | 4.14 |
| 27 | 4.62 | 2.35 | 3.50 | 3.50 | 3.50 | 3.50 | 3.82 | 4.14 |
| 26 | 4.08 | 2.35 | 3.50 | 3.50 | 3.50 | 3.50 | 3.82 | 4.14 |
| 25 | 3.68 | 2.35 | 3.50 | 3.50 | 3.50 | 3.50 | 3.82 | 4.14 |
| 24 | 3.18 | 2.35 | 3.50 | 3.50 | 3.50 | 3.50 | 3.82 | 4.14 |
| 23 | 2.82 | 2.35 | 3.50 | 3.50 | 3.50 | 3.50 | 3.82 | 4.14 |
| 22 | 4.01 | 2.00 | 2.50 | 2.82 | 3.14 | 3.46 | 3.78 | 4.10 |
| 21 | 3.54 | 2.00 | 2.50 | 2.82 | 3.14 | 3.46 | 3.78 | 4.10 |
| 20 | 3.21 | 2.00 | 2.50 | 2.82 | 3.14 | 3.46 | 3.78 | 4.10 |
| 19 | 2.78 | 2.00 | 2.50 | 2.82 | 3.14 | 3.46 | 3.78 | 4.10 |
| 18 | 2.47 | 2.00 | 2.50 | 2.82 | 3.14 | 3.46 | 3.78 | 4.10 |
| 17 | 3.25 | 1.60 | 2.75 | 3.00 | 3.32 | 3.64 | 3.96 | 4.28 |
| 16 | 2.88 | 1.60 | 2.75 | 3.00 | 3.32 | 3.64 | 3.96 | 4.28 |
| 15 | 2.61 | 1.60 | 2.75 | 3.00 | 3.32 | 3.64 | 3.96 | 4.28 |
| 14 | 2.27 | 1.60 | 2.75 | 3.00 | 3.32 | 3.64 | 3.96 | 4.28 |
| 13 | 2.02 | 1.60 | 2.75 | 3.00 | 3.32 | 3.64 | 3.96 | 4.28 |
| 12 | 2.44 | 1.20 | 3.00 | 3.00 | 3.32 | 3.64 | 3.96 | 4.28 |
| 11 | 2.16 | 1.20 | 3.00 | 3.00 | 3.32 | 3.64 | 3.96 | 4.28 |
| 10 | 1.96 | 1.20 | 3.00 | 3.00 | 3.32 | 3.64 | 3.96 | 4.28 |
| 9 | 1.70 | 1.20 | 3.00 | 3.00 | 3.32 | 3.64 | 3.96 | 4.28 |
| 8 | 1.52 | 1.20 | 3.00 | 3.00 | 3.32 | 3.64 | 3.96 | 4.28 |
| 7 | 1.42 | 1.20 | 3.00 | 3.00 | 3.32 | 3.64 | 3.96 | 4.28 |
| 6 | 1.32 | 1.20 | 3.00 | 3.00 | 3.32 | 3.64 | 3.96 | 4.28 |
| 5 | 1.12 | 1.20 | 3.00 | 3.00 | 3.32 | 3.64 | 3.96 | 4.28 |
| 4 | 1.09 | 1.20 | 3.00 | 3.00 | 3.32 | 3.64 | 3.96 | 4.28 |
| 3 | 0.789 | 1.20 | 3.00 | 3.00 | 3.32 | 3.64 | 3.96 | 4.28 |
| 2 | 0.669 | 1.20 | 3.00 | 3.00 | 3.32 | 3.64 | 3.96 | 4.28 |
| 1 | 0.545 | 1.00 | 3.00 | 3.00 | 3.32 | 3.64 | 3.96 | 4.28 |

[†] Nominal values at beginning of life

References

- ¹Rayman, M. D., "The Successful Conclusion of the Deep Space 1 Mission: Important Results Without a Flashy Title," *Space Technology*, Vol. 23, pp. 185-196, 2003.
- ²Lee, M., Weidner, R. J., and Soderblom, L. A., "Deep Space 1 Mission and Observation of Comet Borrelly," *Deep Space 1 Mission and Observation of Comet Borrelly, 45th IEEE International Midwest Symposium on Circuits and Systems*, Tulsa, OK, Aug. 4, 2002.
- ³Polk, J. E., *et al.*, "Performance of the NSTAR Ion Propulsion System on the Deep Space One Mission," AIAA-2001-0965, *39th AIAA Aerospace Sciences Meeting and Exhibit Joint Propulsion Conference*, Reno, NV, January 8-11, 2001.
- ⁴Brophy, J. R., Garner, C., and Mikes, S., "Dawn Ion Propulsion System- Initial Checkout after Launch," AIAA-2008-4917, *44th AIAA/ASME/SAE/ASEE Joint Propulsion Conference & Exhibit*, Hartford, CT, July 20-23, 2008.
- ⁵Herman, D. A., Soulas, G. C., and Patterson, M. J., "Performance Evaluation of the Prototype-Model NEXT Ion Thruster," AIAA-2007-5212 and NASA/TM-2008-215029, *43rd AIAA/ASME/SAE/ASEE Joint Propulsion Conference and Exhibit*, Cincinnati, OH, July 8-11, 2007.
- ⁶Pinero, L. R., Todd, P., and Hopson, M., "Integration and Qualification of the NEXT Power Processing Unit," AIAA-2007-5214, *43rd AIAA/ASME/SAE/ASEE Joint Propulsion Conference and Exhibit*, Cincinnati, OH, July 8-11, 2007.
- ⁷Patterson, M. J. and Benson, S. W., "NEXT Ion Propulsion System Development Status and Capabilities," *Conference Proceedings and NASA/TM-2008-214988, 2007 NASA Science Technology Conference*, College Park, MD, June 19 - 21, 2007.
- ⁸Snyder, J. S., *et al.*, "Vibration Test of a Breadboard Gimbal for the NEXT Ion Engine," AIAA-2006-4665, *42nd AIAA/ASME/SAE/ASEE Joint Propulsion Conference and Exhibit*, Sacramento, CA, July 9-12, 2006.
- ⁹Aadland, R. S., *et al.*, "Development Status of the NEXT Propellant Management System," AIAA-2004-3974, *40th AIAA/ASME/SAE/ASEE Joint Propulsion Conference and Exhibit*, Fort Lauderdale, FL, July 11-14, 2004.
- ¹⁰Hoskins, W. A., *et al.*, "Development of a Prototype Model Ion Thruster for the NEXT System," AIAA-2004-4111, *40th AIAA/ASME/SAE/ASEE Joint Propulsion Conference and Exhibit*, Fort Lauderdale, FL, July 11-14, 2004.
- ¹¹Monheiser, J., Aadland, R. S., and Wilson, F., "Development of a Ground Based Digital Control Interface Unit (DCIU) for the NEXT Propulsion System," AIAA-2004-4112, *40th AIAA/ASME/SAE/ASEE Joint Propulsion Conference and Exhibit*, Fort Lauderdale, FL, July 11-14, 2004.
- ¹²Soulas, G. C., *et al.*, "NEXT Single String Integration Test Results," AIAA-2009-4816, *45th AIAA/ASME/SAE/ASEE Joint Propulsion Conference & Exhibit*, Denver, CO, Aug. 2-5, 2009.
- ¹³Benson, S. W., Patterson, M. J., and Snyder, J. S., "NEXT Ion Propulsion System Progress Towards Technology Readiness," AIAA-2008-5285, *44th AIAA/ASME/SAE/ASEE Joint Propulsion Conference & Exhibit*, Hartford, CT, July 20-23, 2008.
- ¹⁴Pinero, L. R., Hopson, M., Todd, P. C., and Wong, B., "Performance of the NEXT Engineering Model Power Processing Unit," AIAA-2007-5214, *43rd AIAA/ASME/SAE/ASEE Joint Propulsion Conference and Exhibit*, Cincinnati, OH, July 8-11, 2007.
- ¹⁵Anderson, J. R., Snyder, J. S., Van Noord, J. L., and Soulas, G. C., "Thermal Development Test of the NEXT PM1 Ion Engine," AIAA-2007-5217, *43rd AIAA/ASME/SAE/ASEE Joint Propulsion Conference and Exhibit*, Cincinnati, OH, July 8-11, 2007.
- ¹⁶Snyder, J. S., Anderson, J. R., Van Noord, J. L., and Soulas, G. C., "Environmental Testing of the NEXT PM1 Ion Engine," AIAA-2007-5275, *43rd AIAA/ASME/SAE/ASEE Joint Propulsion Conference and Exhibit*, Cincinnati, OH, July 8-11, 2007.
- ¹⁷Patterson, M. J., *et al.*, "NEXT Multi-Thruster Array Test - Engineering Demonstration," AIAA-2006-5180, *42nd AIAA/ASME/SAE/ASEE Joint Propulsion Conference and Exhibit*, Sacramento, CA, July 9-12, 2006.
- ¹⁸Foster, J. E., *et al.*, "Plasma Characteristics Measured in the Plume of a NEXT Multi-Thruster Array," AIAA-2006-5181, *42nd AIAA/ASME/SAE/ASEE Joint Propulsion Conference and Exhibit*, Sacramento, CA, July 9-12, 2006.
- ¹⁹Aadland, R. S., Frederick, H., Benson, S. W., and Malone, S. P., "Development Results of the NEXT Propellant Management System," JANNAF 2005-0356DW, *JANNAF 2nd Liquid Propulsion Subcommittee and 1st Spacecraft Propulsion Subcommittee Joint Meeting*, Monterey, CA, December 5-8, 2005.
- ²⁰Patterson, M. J., Pinero, L. R., Aadland, R., and Komm, D., "NEXT Ion Propulsion System: Single-String Integration Test Results," *JANNAF Proceedings*, Las Vegas, NV, May, 2004.

- ²¹Soulas, G. C., *et al.*, "NEXT Ion Engine 2000 Hour Wear Test Results," AIAA-2004-3791, 40th AIAA/ASME/SAE/ASEE Joint Propulsion Conference and Exhibit, Fort Lauderdale, FL, July 11-14, 2004.
- ²²Van Noord, J. L., "Lifetime Assessment of the NEXT Ion Thruster," AIAA-2007-5274, 43rd AIAA/ASME/SAE/ASEE Joint Propulsion Conference and Exhibit, Cincinnati, OH, July 8-11, 2007.
- ²³Herman, D. A., Pinero, L. R., and Sovey, J. S., "NASA's Evolutionary Xenon Thruster (NEXT) Component Verification Testing," AIAA-2008-4812, 44th AIAA/ASME/SAE/ASEE Joint Propulsion Conference and Exhibit, Hartford, CT, July 21-23, 2008.
- ²⁴Van Noord, J. L. and Herman, D. A., "Application of the NEXT Ion Thruster Lifetime Assessment to Thruster Throttling," AIAA-2008-4526, 44th AIAA/ASME/SAE/ASEE Joint Propulsion Conference and Exhibit, Hartford, CT, July 21-23, 2008.
- ²⁵Herman, D. A., Soulas, G. C., and Patterson, M. J., "NEXT Long-Duration Test after 11,570 h and 237 kg of Xenon Processed," IEPC-2007-033, 30th International Electric Propulsion Conference, Florence, Italy, Sept. 17-20, 2007.
- ²⁶Herman, D. A., Soulas, G. C., and Patterson, M. J., "NEXT Long-Duration Test Plume and Wear Characteristics after 16,550 h of Operation and 337 kg of Xenon Processed," AIAA-2008-4919, 44th AIAA/ASME/SAE/ASEE Joint Propulsion Conference and Exhibit, Hartford, CT, July 21-23, 2008.
- ²⁷Herman, D. A., Soulas, G. C., and Patterson, M. J., "Performance Characteristics of the NEXT Long-Duration Test after 16,550 h and 337 kg of Xenon Processed," AIAA-2008-4527, 44th AIAA/ASME/SAE/ASEE Joint Propulsion Conference and Exhibit, Hartford, CT, July 21-23, 2008.
- ²⁸Patterson, M. J. and Benson, S. W., "NEXT Ion Propulsion System Development Status and Performance," AIAA-2007-5199, 43rd AIAA/ASME/SAE/ASEE Joint Propulsion Conference and Exhibit, Cincinnati, OH, July 8-11, 2007.
- ²⁹Soulas, G. C. and Patterson, M. J., "NEXT Ion Thruster Performance Dispersion Analyses," AIAA-2007-5213, 43rd AIAA/ASME/SAE/ASEE Joint Propulsion Conference and Exhibit, Cincinnati, OH, July 8-11, 2007.
- ³⁰Soulas, G. C., Domonkos, M. T., and Patterson, M. J., "Performance Evaluation of the NEXT Ion Engine," AIAA-2003-5278, 39th AIAA/ASME/SAE/ASEE Joint Propulsion Conference and Exhibit, Huntsville, AL, July 20-23, 2003.
- ³¹Patterson, M. J., *et al.*, "NEXT: NASA's Evolutionary Xenon Thruster," AIAA-2002-3832, 38th AIAA/ASME/SAE/ASEE Joint Propulsion Conference and Exhibit, Indianapolis, IN, July 7-10, 2002.
- ³²Frandina, M. M., *et al.*, "Status of the NEXT Ion Thruster Long Duration Test," AIAA-2005-4065, 41st AIAA/ASME/SAE/ASEE Joint Propulsion Conference and Exhibit, Tucson, AZ, July 10-13, 2005.
- ³³Patterson, M. J., *et al.*, "Plasma Contactor Development for Space Station," IEPC Paper 93-246, 23rd International Electric Propulsion Conference, Seattle, WA, Sept. 13-16, 1993.
- ³⁴Kamhawi, H. and Patterson, M. J., "Update on the Operation Status of the International Space Station Plasma Contactor Hollow Cathode Assemblies," AIAA-2007-5190, 43rd AIAA/ASME/SAE/ASEE Joint Propulsion Conference and Exhibit, Cincinnati, OH, July 8-11, 2007.
- ³⁵Carpenter, C. B., "On the Operational Status of the ISS Plasma Contactor Hollow Cathodes," AIAA-2004-3425, 40th AIAA/ASME/SAE/ASEE Joint Propulsion Conference and Exhibit, Fort Lauderdale, FL, July 11-14, 2004.
- ³⁶Kovaleski, S. D., Patterson, M. J., Soulas, G. C., and Sarver-Verhey, T. R., "A Review of Testing of Hollow Cathodes for the International Space Station Plasma Contactor," IEPC-2001-271, 27th International Electric Propulsion Conference, Pasadena, CA, October 15-19, 2001.
- ³⁷Sarver-Verhey, T. R., "28,000 hour Xenon Hollow Cathode Life Test Results," NASA CR-97-206231 and IEPC Paper 97-0168, 25th International Electric Propulsion Conference, Cleveland, OH, August 24-28, 1997.
- ³⁸Hickman, T. A., Arrington, L. A., Frandina, M. M., and Soulas, G. C., "Overview of the Diagnostics for the NEXT Long Duration Test," AIAA-2005-4064, 41st AIAA/ASME/SAE/ASEE Joint Propulsion Conference and Exhibit, Tucson, AZ, July 10-13, 2005.
- ³⁹Kamhawi, H., Soulas, G. C., and Patterson, M., "NEXT Ion Engine 2000 hour Wear Test Plume and Erosion Results," AIAA-2004-3792, 40th AIAA/ASME/SAE/ASEE Joint Propulsion Conference and Exhibit, Fort Lauderdale, FL, July 11-14, 2004.
- ⁴⁰Brophy, J. R., *et al.*, "The Ion Propulsion System for Dawn," AIAA-2003-4542, 39th AIAA/ASME/SAE/ASEE Joint Propulsion Conference and Exhibit, Huntsville, AL, July 20-23, 2003.
- ⁴¹Brophy, J. R., *et al.*, "Status of the Dawn Ion Propulsion System," AIAA-2004-3433, 40th AIAA/ASME/SAE/ASEE Joint Propulsion Conference and Exhibit, Fort Lauderdale, FL, July 11-14, 2004.
- ⁴²Sengupta, A., *et al.*, "The 30,000-Hour Extended-Life Test of the Deep Space 1 Flight Spare Ion Thruster," NASA/TP 2004-213391, The Jet Propulsion Laboratory and NASA Glenn Research Center, Pasadena, March, 2005.

⁴³Myers, R. M., "Proceedings of the Nuclear Electric Propulsion Workshop, Volume 1: Introductory Material and Thruster Concepts, Section: "MPD Thruster Technology", " JPL D-9512 Vol. 1, June 19-22, 1990.

⁴⁴Sarver-Verhey, T. R. and Soulas, G. C., "International Space Station Cathode Heater Life Testing Results," NASA Glenn Research Center, Cleveland, OH, 1996.

⁴⁵Sengupta, A., *et al.*, "An Overview of the Results from the 30,000 Hr Life Test of Deep Space 1 Flight Spare Engine," AIAA-2004-3608, *40th AIAA/ASME/SAE/ASEE Joint Propulsion Conference and Exhibit*, Fort Lauderdale, FL, July 11-14, 2004.

⁴⁶Mikellides, I., *et al.*, "Neutralizer Hollow Cathode Simulations and Comparisons with Ground Test Data," IEPC-2009-20, *31st International Electric Propulsion Conference*, Ann Arbor, MI, September 20-24, 2009.

⁴⁷Mikellides, I. and Katz, I., "Wear Mechanisms in Electron Sources for Ion Propulsion, I: Neutralizer Hollow Cathode," *Journal of Propulsion and Power*, Vol. 24, No. 4, pp. 855-865, July-August 2008.

⁴⁸Mikellides, I., *et al.*, "Wear Mechanisms in Electron Sources for Ion Propulsion, II: Discharge Hollow Cathode," *Journal of Propulsion and Power*, Vol. 24, No. 4, pp. 866-879, July-August 2008.

⁴⁹Van Noord, J. L., Soulas, G. C., and Sovey, J. S., "NEXT PM1R Ion Thruster and Propellant Management System Wear Test Results," IEPC-2009-163, *31st International Electric Propulsion Conference*, Ann Arbor, MI, September 20-24, 2009.

⁵⁰Polk, J. E., *et al.*, "An Overview of the Results from an 8200 Hour Wear Test of the NSTAR Ion Thruster," AIAA-1999-2446, *35th AIAA/ASME/SAE/ASEE Joint Propulsion Conference and Exhibit*, Los Angeles, CA, June 20-24, 1999.